# NORSAR

ROYAL NORWEGIAN COUNCIL FOR SCIENTIFIC AND INDUSTRIAL RESEARCH

Scientific Report No. 2-82/83

# SEMIANNUAL TECHNICAL SUMMARY
# 1 October 1982 — 31 March 1983

Linda B. Tronrud (ed.)

Kjeller, June 1983

**APPROVED FOR PUBLIC RELEASE, DISTRIBUTION UNLIMITED**

## VI. SUMMARY OF TECHNICAL REPORTS/PAPERS PREPARED

### VI.1 The absorption band effect on long-period body waves

It is generally appreciated that the effect of anelastic absorption on body wave amplitudes is most pronounced in the short-period band. However, in the presence of an absorption band in the mantle, the accompanying velocity dispersion is best observed in long-period body waves. This is because (1) dispersion represents an integral form of $Q^{-1}$ in the band (in contrast to attenuation which represents a 'point property'), and (2) the mantle absorption band extends throughout the long-period range, but not throughout the short-period range of body waves. The last statement is an inference drawn by several authors in recent years, and it is confirmed in the present study. In this work the possibility is explored to use both the dispersion and the amplitude information in a procedure to separate absorption and source effects, and the procedure is applied to SRO/ASRO records of P waves from moderately sized deep focus events between 30 and 90°. The observations were compared to a synthetic purely elastic response, and the observed short-period onset was used to adjust the start time of the synthetic. The last procedure eliminates the effect of station residuals. The implicit assumption here is that the visible short-period onset is unaffected by the absorption; this can be justified later by the results of the analysis. The data are shown in Fig. VI.1.1; other information can be found in Doornbos (1983).

In all examples the long-period waveform is essentially delayed with respect to the synthetic, and the peak amplitude delay is used as an observational parameter. The delay must be explained as the combined effect of the source pulse and the anelastic dispersion. Since dispersion is relatively insensitive to details of an absorption model, we choose a convenient model: the relaxation model which is uniform in $\ell n\tau$, within certain bounds $\tau_1$, $\tau_2$ (Liu, Kanamori and Anderson, 1976):

$$Q^{-1}(\omega) \sim 2\ \mathrm{tg}^{-1} \left\{\frac{\omega(\tau_2-\tau_1)}{1+\omega^2\tau_1\tau_2}\right\} \qquad (1)$$

Our measure of phase velocity dispersion is:

$$D(\omega) = c_\infty c(\omega)-1 \simeq \overline{Q^{-1}(\omega)} \tag{2}$$

where $c_\infty$ and $c(\omega)$ are phase velocities at infinite frequency and at $\omega$, and the overbar denotes the Hilbert transform. For the model (1):

$$D(\omega) \sim \ell n(\tau_2/\tau_1)-\tfrac{1}{2}\ \ell n\left(\frac{1+\omega^2\tau_2^2}{1+\omega^2\tau_1^2}\right) \tag{3}$$

This model is convenient, since the resulting damping and dispersion become explicitly independent of the long-period cut-off $\tau_2$, for $\omega\tau_2 >> 1$. If also $\tau_2 >> \tau_1$:

$$Q^{-1}(\omega) \simeq 2/\pi\ Q_m^{-1} tg^{-1}(1/\omega\tau_1),\quad D(\omega) \simeq \pi/2\ Q_m^{-1}\ \ell n(1+1/\omega^2\tau_1^2)$$

There is good evidence that $\omega\tau_2 >> 1$ at body wave frequencies (Anderson and Given, 1982). The second condition $\tau_2 >> \tau_1$ can be justified a posteriori. It sets the normalizing constant in equation (4) to $\pi$. In the present treatment we have further specified the model by assuming that $Q_m^{-1}$ is given by PREM (which incorporates a long-period Q model). There is then one undetermined parameter $\tau_1$.

In treating the source effect two approaches can be taken. The first is to ignore the effect, i.e., treat the source pulse as a delta function. It results in a maximum estimate for the cut-off frequency of the absorption band, i.e., an absolute minimum for $\tau_1$. In the second approach we adopt a model for the source pulse and estimate the source and absorption parameters simultaneously. It is done by computing the RMS amplitude error, and the time residue, as a function of trial cut-off relaxation time $\tau_1$.

The results of this experiment are shown in Fig. VI.1.2. The time residue and RMS error curve are consistent, and zero time residue corresponds to an absorption bandwidth near 0.2 Hz, i.e., $\tau_1$ near 0.9 s. In the presence of noise and in the context of a single absorption band this constraint can be somewhat relaxed, and cut-off frequencies up to 1 Hz are admitted by the data. The result represents the integrated effect of $Q^{-1}$ along the wave path but it can be directly applied to correct body waves synthesized in purely elastic, or frequency independent Q, models. Since the present result is based on teleseismic records from deep events, it should be more representative of absorption in the lower mantle.

D.J. Doornbos

## References

Anderson, D.L. and J.W. Given (1982): Absorption band Q model for the earth, J. Geophys. Res. 87, 3893-3904.

Doornbos, D.J. (1983): Observable effects of the seismic absorption band in the earth. Submitted for publication.

Liu, H.P., D.L. Anderson and H. Kanamori (1976): Velocity dispersion due to anelasticity: implications for seismology and mantle composition, Geophys. J.R. Astr. Soc. 47, 41-58.

Fig. VI.1.1 Observed short-period P wave (upper trace, record length 12 seconds), observed and synthetic long-period P wave (middle and lower trace, record length 60 seconds). The anelastic absorption effect is deleted from the synthetic, and note the time delay between the observed and synthetic waveform. Observations are numbered according to Doornbos (1983).

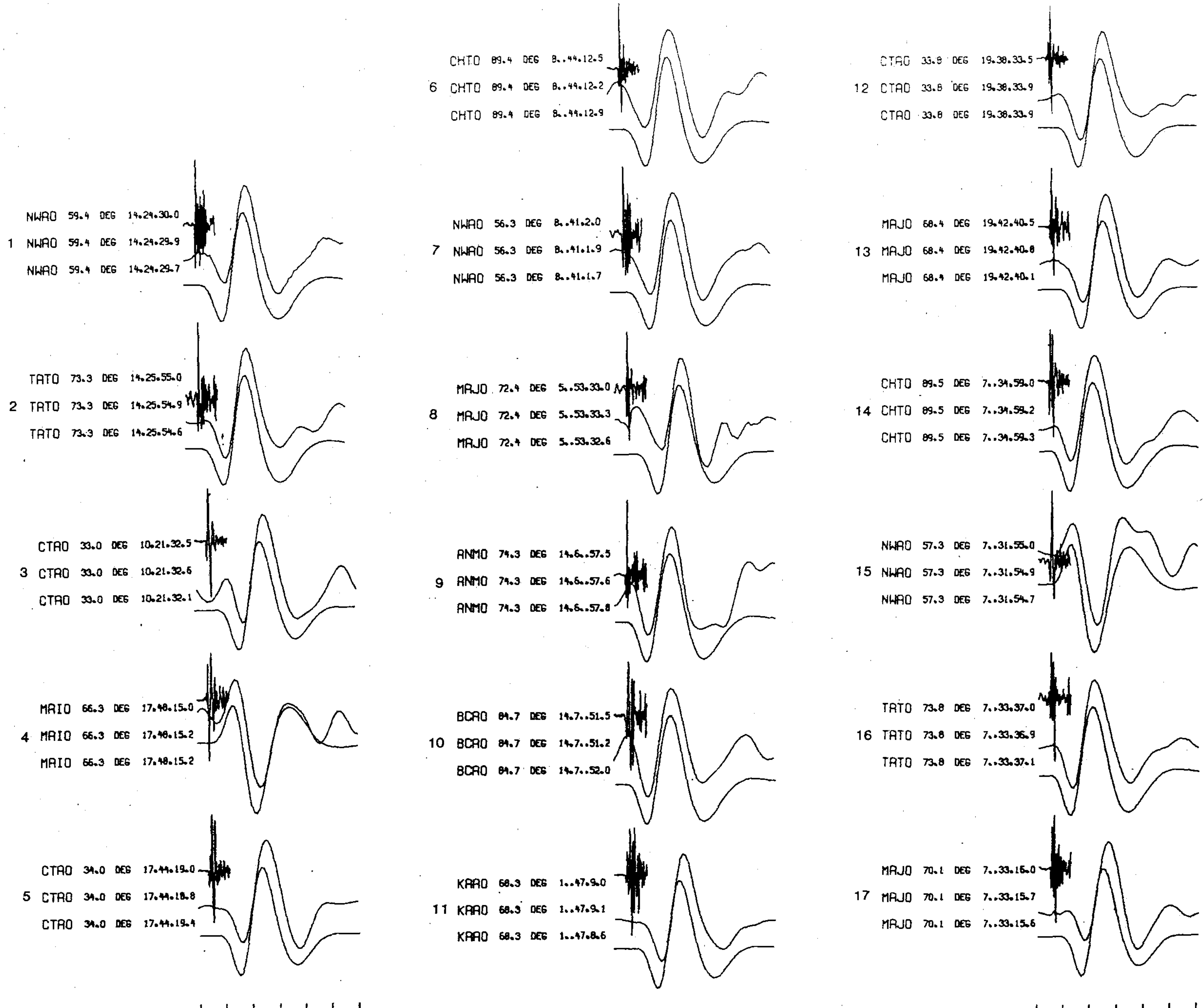

NWAO 59.4 DEG 14.24.30.0
1 NWAO 59.4 DEG 14.24.29.9
NWAO 59.4 DEG 14.24.29.7
TATO 73.3 DEG 14.25.55.0
2 TATO 73.3 DEG 14.25.54.9
TATO 73.3 DEG 14.25.54.6
CTAO 33.0 DEG 10.21.32.5
3 CTAO 33.0 DEG 10.21.32.6
CTAO 33.0 DEG 10.21.32.1
MAIO 66.3 DEG 17.48.15.0
4 MAIO 66.3 DEG 17.48.15.2
MAIO 66.3 DEG 17.48.15.2
CTAO 34.0 DEG 17.44.19.0
5 CTAO 34.0 DEG 17.44.18.8
CTAO 34.0 DEG 17.44.19.4
CHTO 89.4 DEG 8..44.12.5
6 CHTO 89.4 DEG 8..44.12.2
CHTO 89.4 DEG 8..44.12.9
NWAO 56.3 DEG 8..41.2.0
7 NWAO 56.3 DEG 8..41.1.9
NWAO 56.3 DEG 8..41.1.7
MAJO 72.4 DEG 5..53.33.0
8 MAJO 72.4 DEG 5..53.33.3
MAJO 72.4 DEG 5..53.32.6
ANMO 74.3 DEG 14.6..57.5
9 ANMO 74.3 DEG 14.6..57.6
ANMO 74.3 DEG 14.6..57.8
BCAO 84.7 DEG 14.7..51.5
10 BCAO 84.7 DEG 14.7..51.2
BCAO 84.7 DEG 14.7..52.0
KAAO 68.3 DEG 1..47.9.0
11 KAAO 68.3 DEG 1..47.9.1
KAAO 68.3 DEG 1..47.8.6
CTAO 33.8 DEG 19.38.33.5
12 CTAO 33.8 DEG 19.38.33.9
CTAO 33.8 DEG 19.38.33.9
MAJO 68.4 DEG 19.42.40.5
13 MAJO 68.4 DEG 19.42.40.8
MAJO 68.4 DEG 19.42.40.1
CHTO 89.5 DEG 7..34.59.0
14 CHTO 89.5 DEG 7..34.59.2
CHTO 89.5 DEG 7..34.59.3
NWAO 57.3 DEG 7..31.55.0
15 NWAO 57.3 DEG 7..31.54.9
NWAO 57.3 DEG 7..31.54.7
TATO 73.8 DEG 7..33.37.0
16 TATO 73.8 DEG 7..33.36.9
TATO 73.8 DEG 7..33.37.1
MAJO 70.1 DEG 7..33.16.0
17 MAJO 70.1 DEG 7..33.15.7
MAJO 70.1 DEG 7..33.15.6

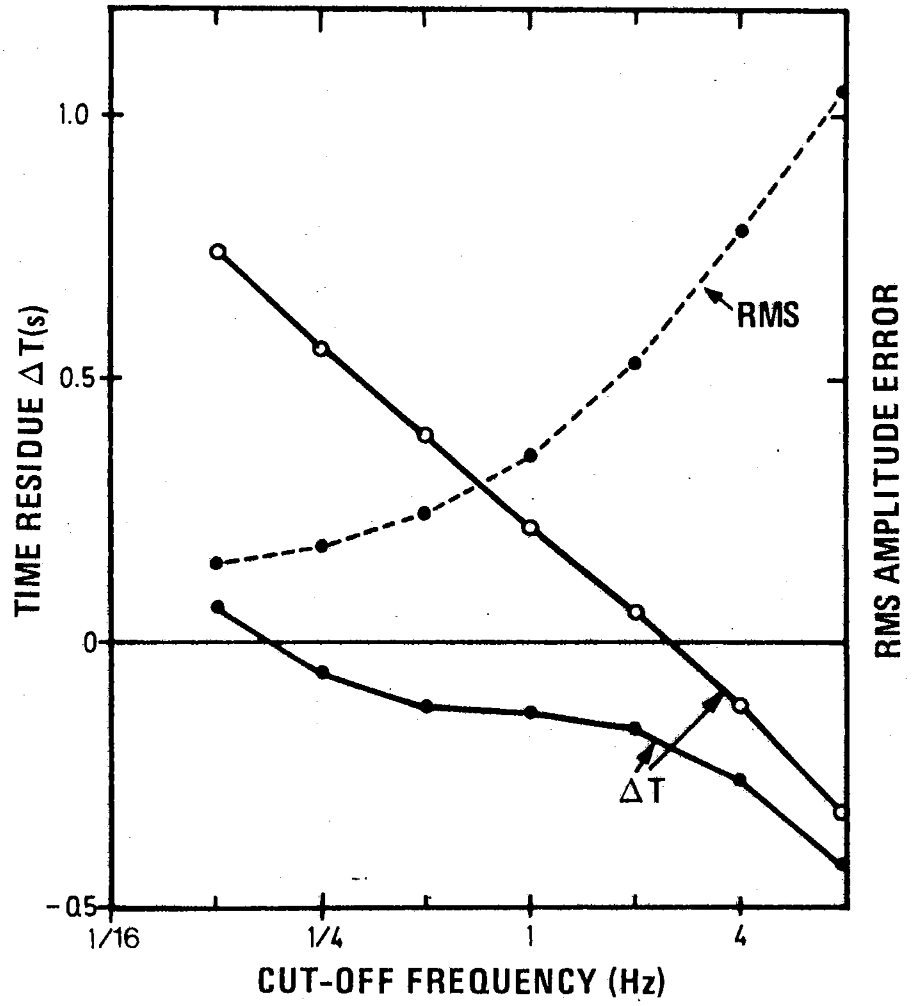


Fig. VI.1.2 Averaged time residue and RMS amplitude error in fitting a source and absorption model to the P wave data of Fig. VI.1.1, as a function of the high-frequency cut-off of the absorption band. The closed dots represent a solution with finite source effect. The open dots represent a solution where the source effect is ignored.